Живот ван домовине

Ненад Вукичевић, потпредседник

Српски конгрес уједињења

До сада сте вероватно већ прочитали доста материјала о професору Марку Јарићу, тако да се ја не бих упуштао у навођења бројних награда и публикација које је професор Јарић објавио. Морам само да нагласим да су радови професора Јарића у области квазикристала једни од највише цитираних у свету. Он је био пионир истраживања о квазикристалима, о којима је објавио и серију књига. Током свог живота показао се као велики таленат и стручњак у свим областима у којима је радио, што показују и бројне награде и стипендије које је добио.

С обзиром да је Марко Јарић живео у Америци, хтео бих да се осврнем на његов друштвени живот ван домовине. Упознао сам га 1991. године на Стенфорд Универзитету (Stanford University), где смо заједно присуствовали једној расправи о догађајима у Југославији. Био сам веома импресиониран Марковим коментарима и аргументима у расправи, тако да сам му морао прићи, да би се упознали. Временом, постали смо блиски пријатељи. Од тада је професор Јарић био један од организатора свих демонстрација у Сан Франсиску против санкција које су Југославији уведене, и неколико пута је учествовао на локалним телевизијским каналима, објашњавајући у чему је проблем. Једном је чак и био гост у емисији Националног радија, која је била посвећена Југославији. Други учесник у емисији је био сенатор Лантош, који је отворено заговарао антисрпску политику. Професор Јарић је са лакоћом и аргументовано одбацио све његове тврдње, и оставио је врло добар утисак на слушаоце.

У последњих неколико година живота више пута је жртвовао публиковање својих научних радова, јер издавач није хтео да штампа све титуле које је професор Јарић имао. Наиме, од 1993. године он је постао професор на факултету "Никола Тесла" у Книну, што је увек и са поносом истицао. Адресу факултета је наводио као Република Српска Крајина, што је некоме у самом врху Америчког физичког друштва веома сметало. Због овога је професор Јарић водио велику борбу са издавачем, да би после неколико недеља одбио да штампа рад у најтиражнијем листу за физику коју издаје Америчко Физичко друштво. Међутим, последњи рад у водећем часопису за физику, Physical Review Letters, у 1994. години, Марко је, ипак, успео да објави са потпуном адресом.

На крају, морам да напоменем да је професор Јарић увек био у вези са домовином по патриотској и професионалној линији. Током свог дугогодишњег рада по универзитетима широм Америке обезбедио је бројне стипендије нашим надареним постдипломским студентима, као и посете и предавања стручњацима и професорима из домовине. Остаје нам да дубоко жалимо што је прерана смрт прекратила једну блиставу научну каријеру.

World Class Scientist

Joseph L. Birman, Distinguished Professor

Department of Physics, City College of New York,
New York, NY10031, USA

Marko Jarić has been a world class theoretical physicist with specialization in original scientific work on condensed matter theory, and on biophysics. I have followed his scientific work very closely for about 25 years, since he first came to the City College of City University of New York, to pursue his work toward the Ph.D. He wrote his Ph.D. thesis under my mentorship, and we have been in close touch thereafter. His first work, with me, was a deep study of the group theoretical symmetry effects embedded in the Renormalization Group Programme for second order phase transitions. This was path-breaking work in my opinion, which has laid the groundwork for additional studies on the group theory aspects of the recursive renormalization procedure, and the significance of the approach to fixed points manifesting some new dynamical symmetry. Marko discovered sets of symmetry related fixed points and he was able to analyze them, and determine in some cases certain "selection rules" which constrain the allowed set of fixed points. While still a graduate student Marko deepened and generalized my earlier work on the "Chain Criterion" for symmetry-breaking in a series of successive second order phase transitions. Again in this work he grasped an essential new point (which I had earlier overlooked) and was able to put it into precise mathematical terms where it can be applied. This criterion has been widely used in studies of successive phase transitions (see the monographs by Jerszy Kocinski "Theory of Symmetry Changes at Continuous Phase Transitions" (Elsevier Press, 1983); and Jerszy Kocinski "Commensurate & Incommensurate Phase Transitions" (Elsevier Press, 1990)).

The arc of his creativity continued to rise quickly, as he turned his attention to two important topics: the theory of quasicrystals and the theory of crystallization. His original work on quasicrystals continued the general theme of symmetry, insofar as he exhaustively studied the underlying icosahedral symmetry group for quasicrystals. He determined the mathematical invariants and the complete set of basis functions for this group—surprisingly this had never been done before, despite the formal knowledge for more than a century that the icosahedral group is one of the discrete subgroups of the

three-dimensional isotropy group. The result of this investigation was a major paper, co-authored by L. Michel and R. Sharp, which is a landmark work of immediate relevance and use to any investigator of quascrystals. I might note that as a side effect of Marko's investigation of the icosahedral symmetry group, he was able to quickly solve an important problem relating to the possible appearance of "hexatic" phase in an icosahedral quasicrystal system. This last problem had occupied Professor David Nelson of Harvard for some time and he was "astonished" (he informed me) at how quickly Marko solved this difficult problem. Marko simultaneously investigated the physics of defects in quasicrystals and determined the relative stability of several of the general types against merger, or against disappearance into the bulk. This work led to his major studies on the totally novel type of elementary lattice distortion in such media–now known as "phason" disorder. Marko's work permitted the experimenters to carefully analyze the complicated scattering patterns and to quantitatively estimate the quantity of phason disorder which is present.

After a period of slow growth (in the early 1990's) the topic of quasicrystal physics is now set for a new major push forward, in large part due to the availability of large cm–size materials. Marko's work, with his students at Texas, has provided the tools by which this new generation of materials can be classified as to their structural purity. As I recently learned from Professor Danni Schechtmann of the Technion (a co-discoverer of quasicrystals) when I visited him in January of 1998, the new generation of quasicrystals is even finding use in kitchen cookware (as linings for cooking utensils), due to their marvelous thermal insulating properties. This heightens the importance of being able to utilize Marko's analysis in practical fashion.

In his work on the theory of melting-crystallization, Marko deeply clarified the conditions needed to form perfect or disordered crystals when, for example a molten metal begins to form the ordered crystalline phase. In this work Marko was able to apply some general theoretical background, due to Ramakrishnan and others, to the concrete problem of melting and crystal growth. The new theory has been a most important tool in hands of modern crystal growers who desire to modify the conditions of concentration, temperature gradient, and cooling rate, in order to produce the largest and most perfect crystal and also quasicrystal.

In recent years, before he was struck by the fatal illness, Marko had returned to an earlier interest in biophysics. His work was focused on the

conditions for the stability of different morphological or structural types for poly-molecules, including polymers. In this work, which in my opinion was brilliantly conceived, he utilized an important–and perhaps surprising–analogy between such biological molecules and the inorganic magnetic, and antiferromagnetic, systems which have been very long studied.

I believe that the above indications of the highlights of Marko Jarić's original scientific contributions merely touches on them. His work was characterized by an unusual ability to penetrate to the vital core of a problem, to extract the essential elements, and then to formulate and exhaustively solve, in proper mathematical fashion, the quantitative analysis of the resulting mathematical models. Out of this work often came a deep and beautiful understanding of the essential physics involved, which Marko was then able to present to the scientific community in an economic and clear fashion. The tragedy of his untimely death at age 45 is that he was now entering the full power of his mature scientific ability, so that we have been deprived of even more brilliant and seminal understanding of the physics of quasicrystals – in which he was an acknowledged world leader – as well as biophysical problems with potential for improving therapeutic functioning of anti-illness medicines.

I want to touch briefly on Marko's superb ability as a teacher. While still in Graduate School, he organized and was the "sparkplug" of a graduate student seminar which engaged all the graduate students in physics at that time. As this seminar evolved, he brought in faculty for some special lectures, but mainly Marko and several of his then contemporaries would review current literature, and the status of their own researches. Marko went on, during his academic career in several academic locations – finally at Texas – to become a very gifted teacher. His students were extremely appreciative of his clear and well-prepared lectures and were attracted to him. His graduate students and all who heard him lecture were taken strongly by the exceptional clarity and enthusiasm of his presentations. In short, he has been able to transfer some of his passion for physics to later generations. I define this as superb teaching ability.

I need also to mention at this point Marko's deep and passionate involvement in the terrible troubles which have befallen his country in recent years. In his last years he put much energy into seeking solutions, proposing them, and working to settle conflict. Another dimension to the tragedy of his death is that his intelligence and creative ability is now lost to those seeking to implement permanent, peaceful, and fair solutions.

In my opinion Marko V. Jarić represents the highest ideal and the highest realization of the ideal of: creative scientist, educator and teacher of his students; a seminal and brilliantly original physicist, and engaged human being in finding solutions to real-world problems.

ČASOPIS
STUDENATA
FIZIKE

FIZIKA

16·17

APRIL 74.
NOVEMBAR 75.

problemi savremene fizike

prevodi

informacije

ZADACI iz fizičke mehanike, fizike II, teorijske mehanike, teorijske fizike i kvantne mehanike

- + - + -

S A D R Ž A J

JEDAN PRIMER HAMILTONIJANA KOJI JE U PROTIVREČNOSTI SA TREĆIM PRINCIPOM TERMODINAMIKE

I

Termodinamika, kao fenomenološka disciplina, daje nam dobro poznate osnovne principe. Jedan od njih je i treći princip termodinamike koji kaže da entropija po jednoj čestici teži nuli kada broj čestica teži beskonačno i temperatura teži nuli. U pojedinim udžbenicima može se naći i nešto drugačije formulisan treći princip termodinamike: kod sistema, čije je osnovno stanje nedegenerisano, entropija po jednoj čestici teži nuli kada broj čestica teži beskonačno, a temperatura teži nuli. Međutim, u okviru statističke mehanike kao teorijske, matematičke discipline moguće je naći primere koji su u protivrečnosti sa ovako formulisanim trećim principom. Tako, na primer, Robert B. Griffiths /1/ navodi da hamiltonijan oblika:

$$\mathcal{H} = J\left[\sum_{i=1}^{N} \sigma_i^2 - \sum_{i=1}^{N-1} (\sigma_i \sigma_{i+1})^2\right], \quad \underset{J>0}{J=\text{const}}, \quad \sigma_i = -1, 0, +1 \tag{1}$$

protivreči trećem principu.

Zaista ovaj hamiltonijan lanca N spinova, koji mogu imati tri projekcije, daje nedegenerisano osnovno stanje $(\mathcal{H}=0 \leftrightarrow \sigma_i=0)$. Da bismo našli kako se ponaša entropija po čestici $\frac{S}{N}$ potražimo prvo statističku sumu sistema:

$$Q^{(N)} \equiv Q(N,T) = \sum_{\sigma_1=-1,0,1} \cdots \sum_{\sigma_N=-1,0,1} e^{-\beta J\left[\sum_{i=1}^{N} \sigma_i^2 - \sum_{i=1}^{N-1} (\sigma_i \sigma_{i+1})^2\right]}; \quad \beta = \frac{1}{kT} \tag{2}$$

Kako svaki spin može imati tri projekcije moguće je ostvariti ukupno 3^N konfiguracija od N spinova. Tako da možemo napisati statističku sumu u obliku:

$$Q^{(N)} = \sum_{j=1}^{3^N} e^{-\beta E_j^{(N)}} \tag{3}$$

gde se sumiranje vrši po svim konfiguracijama.a:

$$E_j^{(N)} = J\left[\sum_{i=1}^{N}{}^{j} \sigma^2 - \sum^{N-1} (\sigma_i \sigma_{i+1})^2\right] \tag{4}$$

$\sum^{j}$ označava da se sumira za neku j-tu konfiguraciju.

Postavimo korespodenciju $-1 \leftrightarrow 0$, $0 \leftrightarrow 1$, $1 \leftrightarrow 2$, tada sve konfiguracije možemo indeksirati na sledeći način:

indeks	konfiguracija
1	000...00
2	000...01
3	000...02
4	000...10
⋮	⋮
3^{N-1}	002...22
$3^{N-1}+1$	010...00
$3^{N-1}+2$	010...01
⋮	⋮
$2\cdot 3^{N-1}$	012...22
$2\cdot 3^{N-1}+1$	020...00
⋮	⋮
3^N	022...22
3^N+1	100...00
⋮	⋮
$2\cdot 3^N$	122...22
$2\cdot 3^N+1$	200...00
⋮	⋮
3^{N+1}	222...22

N

Kada smo ovako indeksirali konfiguracije podelimo $Q^{(N)}$ na tri sume:

$$(5)\quad Q^{(N)} = \sum_{j=1}^{3^{N-1}} e^{-\beta E_j^{(N)}} + \sum_{j=3^{N-1}+1}^{2\cdot 3^{N-1}} e^{-\beta E_j^{(N)}} + \sum_{j=2\cdot 3^{N-1}+1}^{3^N} e^{-\beta E_j^{(N)}} = Q_1^{(N)} + Q_2^{(N)} + Q_3^{(N)}$$

Očigledno je da svaki $E_j^{(N)};\ 1\le j\le 3^{N-1}$ ima jedan i samo jedan sebi odgovarajući $E_j^{(N)};\ 2\cdot 3^{N-1}<j\le 3^N$ koji se dobija smenom $0\to 2$ i $2\to 0$. To odgovara smeni u hamiltonijanu $\sigma_i=-1\to 1$ i $\sigma_i=1\to -1$. Iz oblika hamiltonijana je očigledno da se pri takvoj smeni $E_j^{(N)}$ ne menja, a to znači da je::

$$(6)\quad Q_1^{(N)} = Q_3^{(N)} \equiv \frac{1}{2} Q_1^{(N)}$$

Tako da imamo:

$$(7)\quad Q^{(N)} = Q_1^{(N)} + Q_2^{(N)}$$

Razmotrimo $Q_1^{(N)}$:

$$(8)\quad \frac{1}{2} Q_1^{(N)} = Q_1^{(N)} = \sum_{j=1}^{3^{N-1}} e^{-\beta E_j^{(N)}} = \sum_{j=1}^{3^{N-2}} e^{-\beta E_j^{(N)}} + \sum_{j=3^{N-2}+1}^{2\cdot 3^{N-2}} e^{-\beta E_j^{(N)}} + \sum_{j=2\cdot 3^{N-2}+1}^{3^{N-1}} e^{-\beta E_j^{(N)}}$$

Uočimo sada da je:

$$(9)\quad E_j^{(N)} = \begin{cases} E_j^{(N-1)} & 1\le j\le 3^{N-2} \\ E_j^{(N-1)} + J & 3^{N-2}<j\le 2\cdot 3^{N-2} \\ E_j^{(N-1)} & 2\cdot 3^{N-2}<j\le 3^{N-1} \end{cases}$$

Primenivši (9) dobijamo:

$$\frac{1}{2}\overset{(N)}{Q}_1 = \sum_{j=1}^{3^{N-2}} e^{-\beta \overset{(N-1)}{E_j}} + \sum_{j=3^{N-2}+1}^{2\cdot 3^{N-2}} e^{-\beta(\overset{(N-1)}{E_j}+J)} + \sum_{j=2\cdot 3^{N-2}+1}^{3^{N-1}} e^{-\beta \overset{(N-1)}{E_j}} =$$

(10)

$$= \overset{(N-1)}{Q_1} + e^{-\beta J}\overset{(N-1)}{Q_2} + \overset{(N-1)}{Q_3} = \overset{(N-1)}{Q_1} + e^{-\beta J}\overset{(N-1)}{Q_2}$$

Odnosno:

$$\overset{(N)}{Q_1} = 2\overset{(N-1)}{Q_1} + 2e^{-\beta J}\cdot \overset{(N-1)}{Q_2} \tag{11}$$

Slično se dobija:

$$\overset{(N)}{Q_2} = \overset{(N-1)}{Q_1} + \overset{(N-1)}{Q_2} \tag{12}$$

Napisano matrično i produženo do $\overset{(2)}{Q_1}$, $\overset{(2)}{Q_2}$:

$$\begin{Bmatrix} \overset{(N)}{Q_1} \\ \overset{(N)}{Q_2} \end{Bmatrix} = \begin{Bmatrix} 2 & 2e^{-\beta J} \\ 1 & 1 \end{Bmatrix}^{N-2} \begin{Bmatrix} \overset{(2)}{Q_1} \\ \overset{(2)}{Q_2} \end{Bmatrix} \tag{13}$$

Odavde se dobija za veliko N :

$$\frac{1}{N}\ln \overset{(N)}{Q} \longrightarrow \ln \lambda_1 \tag{14}$$

gde je λ_1 po apsolutnoj vrednosti veća karakteristična vrednost matrice:

$$\begin{Bmatrix} 2 & 2e^{-\beta J} \\ 1 & 1 \end{Bmatrix} \tag{15}$$

I :

$$\lambda_1 = \frac{3}{2} + \sqrt{\frac{1}{4} + 2e^{-\beta J}} \tag{16}$$

Tako da dobijamo:

$$\frac{1}{N}\ln \overset{(N)}{Q} \longrightarrow \ln\left(\frac{3}{2} + \sqrt{\frac{1}{4} + 2e^{-\beta J}}\right) \tag{17}$$

Potražimo $\frac{S}{N}$ za veliko N. Poznato je:

$$\frac{S}{N} = -\frac{1}{N}\frac{\partial F}{\partial T} \tag{18}$$

gde je F slobodna energija. Kako je:

$$F = -kT \ln Q^{(N)} \tag{19}$$

imamo:

$$s \equiv \frac{S}{N} = \frac{k}{N} \frac{\partial T \ln Q^{(N)}}{\partial T} = k \left(\frac{\ln Q^{(N)}}{N} + T \frac{\partial}{\partial T} \frac{\ln Q^{(N)}}{N} \right) \tag{20}$$

Za veliko N dobijamo+:

$$\lim_{N\to\infty} s = k \ln \lambda_1 + kT \frac{\partial}{\partial T} \ln \lambda_1 =$$

$$= k \left[\ln \left(\frac{3}{2} + \sqrt{\frac{1}{4} + 2e^{-3\beta}} \right) + \frac{3\beta e^{-3\beta}}{\left(\frac{3}{2} + \sqrt{\frac{1}{4} + 2e^{-3\beta}} \right) \sqrt{\frac{1}{4} + 2e^{-3\beta}}} \right] \tag{21}$$

Odavde je očigledno:

$$\lim_{T\to 0} \lim_{N\to\infty} s = k \ln 2 > 0 \tag{22}$$

+Kada se eksplicitno zameni izraz za $\ln Q^{(N)}$ vidi se da je moguće:

$$\lim_{N\to\infty} \frac{\partial}{\partial T} \frac{\ln Q^{(N)}}{N} = \frac{\partial}{\partial T} \lim_{N\to\infty} \frac{\ln Q^{(N)}}{N}$$

Literatura

1. Griffiths, R. B. ,The Third Law and Statistical Mechanics, A Critical Review of Thermodynamics,1970.

25.12.1973.
Beograd

JARIĆ MARKO, student IV godine Fizike PMF-a,
Univerzitet u Beogradu

The Computer Magazine for Scientists and Engineers

COMPUTERS IN PHYSICS

MAR/APR 1996

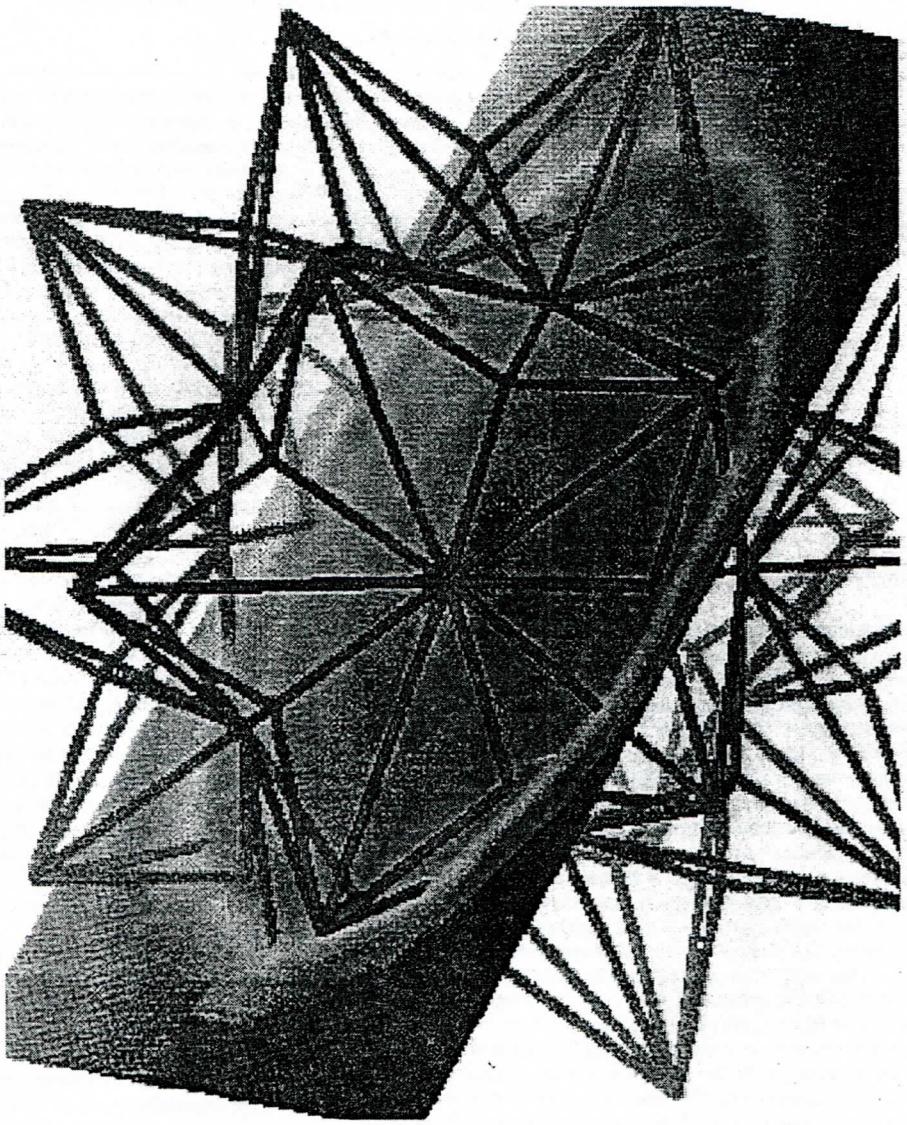

AMERICAN INSTITUTE OF PHYSICS

Analyzing Chemicals
Visualizing Quasicrystals

Visualization and analysis of quasicrystal densities

Shi-Yue Qiu
Department of Physics, Iowa State University, Ames, Iowa 50011

Corbett R. Rowell
Department of Physics, University of California, Santa Cruz, California 95064

Marko Vukobrat Jarić[a)]
Department of Physics, Cornell University, Ithaca, New York 14853-2501
and Department of Physics, Texas A&M University, College Station, Texas 77843-4242

(Received 11 October 1994; accepted 11 September 1995)

Several techniques for visualizing and analyzing scatterer densities of quasiperiodic quasicrystals, both in the physical space and in the associated hyperspace, are discussed. In particular, a method for analyzing quasicrystal densities in terms of tilings is introduced and illustrated for the icosahedral Ammann tiling. A specific application to the x-ray and neutron scattering data of i($Al_{0.570}Cu_{0.108}Li_{0.322}$) is made. The six-dimensional hyperspace density of i($Al_{0.570}Cu_{0.108}Li_{0.322}$) is found to be consistent with the presence of hyperatoms on vertices, edge centers, and body centers of the hypercubic lattice. Some gross features of the hyperatom shapes are suggested. In the physical space, it is shown that densities around some high symmetry points are similar to those in R($Al_{0.564}Cu_{0.116}Li_{0.320}$) crystal, while around others, they suggest new atomic clusters. The Ammann tiling is found to be a useful template for the structure of i($Al_{0.570}Cu_{0.108}Li_{0.322}$), with the rhombic dodecahedra as important building units. While several structural models of i($Al_{0.570}Cu_{0.108}Li_{0.322}$) are generally consistent with the results of the density analysis, some differences are detected. A symmetric decoration of the rhombic dodecahedron, similar to the one found in R($Al_{0.564}Cu_{0.116}Li_{0.320}$), that is a basis for several structural models, is not consistent with the density analysis. No sign of the pure Al inside the rhombic dodecahedra, nor of the related Al hyperatom at the body center of the hypercrystal, could be detected. © *1995 American Institute of Physics.*

INTRODUCTION

Determination of the real space quasicrystal structures from their diffraction data available in the reciprocal space is an important problem in quasicrystal research.[1,2] A real space information about the structure is contained in the Patterson function which can be easily obtained by the Fourier transform of the observed diffraction intensities. Indeed, several authors have constructed and analyzed pair distribution functions (Patterson functions) of various icosahedral and decagonal quasicrystals both in the physical space[3–6] and in the hypothetical hyperspace that is associated with their assumed quasiperiodicity.[6–12] However, since the Patterson function is a density–density autocorrelation function, it does not uniquely fix the actual density of scatterers, significantly limiting the structural information it contains.

This lack of uniqueness can be traced back to the fact that diffraction intensities give only the magnitude of the structure factors, not their phases. However, two methods were developed recently for solving the phase problem and reconstructing structure factors in certain classes of quasiperiodic quasicrystals.[13,14] Therefore, the density of scatterers can be easily determined for such quasicrystals by calculating the Fourier transform of the reconstructed structure factors. Then, the resulting density can be analyzed either in the physical space or in the hyperspace associated with the quasiperiodicity. Because of the lack of periodicity, and because of the so-called "phason" disordering responsible for the occurrence of partial occupancies of sites in quasicrystals, the density analysis in the physical space is most useful when the density can be associated with a packing (tiling) of a relatively small number of clusters (tiles). Then, the density on a tile of a given type needs to be averaged over all appearances of the tile in the structure. However, since a quasiperiodic density can be generally represented as a cut through a higher dimensional periodic density, an analysis in the hyperspace may often be more informative.

An objective of this paper is to summarize the theoretical tools necessary for the analysis of reconstructed quasicrystal densities. In particular, a method for the analysis of quasicrystal densities in terms of tilings will be introduced. These tools will be applied to i($Al_{0.570}Cu_{0.108}Li_{0.322}$), and inferences about its atomic structure will be drawn.

Experimentally, the high resolution transmission electron micrographs (HRTEM) reveal the phase information of the scatterer density, which cannot be obtained from the Patterson function. While the connection between two-

[a)]E-mail: marko@sharac.tamu.edu

0894-1866/96/10(2)/154/20/$10.00

dimensional projections of the reconstructed scatterer densities and the HRTEM images is certainly more complicated, it will be shown that they are in a qualitative agreement for i($Al_{0.570}Cu_{0.108}Li_{0.322}$). This lends a support to the accuracy of the reconstructed phase and encourages further analysis of the reconstructed scatterer densities.

The quasicrystalline i($Al_{0.570}Cu_{0.108}Li_{0.322}$) will be represented by a six-dimensional periodic crystal. An analysis of the reconstructed i($Al_{0.570}Cu_{0.108}Li_{0.322}$) densities in high symmetry hypercrystal planes will reveal that high densities occur mainly along three-dimensional planes parallel to the "inner space," the space orthogonal to the physical space. These high density three-dimensional planes are found centered at vertices (V), edge centers (E), or body centers (B) of the associated hypercubic lattice, hinting that these should be the locations of hyperatoms in a perfectly ordered structure. The density evaluated within these planes will provide clues to the hyperatom compositions and shapes. By considering scatterer densities for both x-ray and neutron diffraction, which we shall simply call electron and nuclear densities, respectively, it will become clear that the chemical composition of V and E hyperatoms must be mainly Al and Cu, while the B hyperatom must be mostly Li. The density will be found reduced at the center of the V site, forming a shell slightly extended along the fivefold symmetry axes. This suggests a hyperatom shape that is close to a slightly rounded icosahedron with a hole at its center. At the E site, the density will suggest an oblate hyperatom shape that is squashed along its fivefold axis with a decagonal cross section and peaks in the directions of the perpendicular twofold axes. The isodensity surfaces at the B site will indicate a shape close to a pentagonal dodecahedron with slighly concave facets perpendicular to the fivefold axes.

The physical space densities will be analyzed primarily in terms of the Ammann tiling. The densities and their rms variances will be evaluated on the average prolate and oblate rhombohedra (PR and OR, respectively) in several types of local environments. It will be evident that the tiles which are inside rhombic dodecahedra (RD) are considerably different from those that are not. Furthermore, based on the size of the variances it will follow that the RD could be considered as an independent tiling unit. While the density analysis will be found generally consistent with the i($Al_{0.570}Cu_{0.108}Li_{0.322}$) atomic structure models of Refs. 15 and 16, some important differences will be identified. Among other differences, it will be shown that the existence of a separate Al hyperatom at B, postulated in the structure model of Ref. 16, but questioned in Ref. 15, is inconsistent with the density reconstructed here.

The remainder of this paper is organized as follows. In Sec. I we present the formalism necessary for the analysis of quasicrystal densities in the hyperspace and in the physical space with a particular emphasis on the Ammann tiling analysis of physical space densities for icosahedral quasicrystals. Then, the results of an application of this formalism to i($Al_{0.570}Cu_{0.108}Li_{0.322}$), and their consequences for the modeling of i($Al_{0.570}Cu_{0.108}Li_{0.322}$), are discussed in Sec. II. The conclusions of this paper are summarized in Sec. III. This work is based in part on the Ph.D. thesis of one of the authors,[17] and on the Senior thesis of another.[18]

I. FORMALISM

A. General

Two recently developed methods facilitate determination of the absolute scale s of the diffraction intensities $I(\mathbf{Q})$ and of the phases $\theta(\mathbf{Q})$ of the structure factors $F(\mathbf{Q})$ for certain classes of quasiperiodic crystals.[13,14] They have been successfully applied to both x-ray and neutron diffraction data of i($Al_{0.570}Cu_{0.108}Li_{0.322}$) quasicrystal.[13,14] Like in the ordinary crystal structure determination, the reconstructed structure factors $F(\mathbf{Q})=s\sqrt{I(\mathbf{Q})}e^{i\theta(\mathbf{Q})}$ can be used as a guide for the quasicrystal structure determination by reconstructing the quasicrystal density of scatterers $\rho(\mathbf{r})$,

$$\rho(\mathbf{r})=\sum_{\mathbf{Q}} F(\mathbf{Q})e^{-i\mathbf{Q}\cdot\mathbf{r}}. \tag{1}$$

Although an analysis of this density can be carried out fully in the physical space, a higher dimensional representation of the density may provide a conceptually simpler picture. Namely, it is well known from the original theory of quasiperiodic functions,[19,20] as well as from its applications to incommensurate crystals[21,22] and quasicrystals,[23–27] that a quasiperiodic function can be represented as a cut through (a restriction of) a periodic function in a higher dimensional space (hyperspace). The reader is directed to the Appendices of Ref. 15 for further description of the construction of the hypercrystal, our notation, and specific coordinate systems[28,29] appropriate for i($Al_{0.570}Cu_{0.108}Li_{0.322}$) that we will use here. The hypercrystal structure factor at the reciprocal hyperlattice vector $\bar{\mathbf{Q}}\equiv(\mathbf{Q},\mathbf{Q}^{\perp})$ is defined by $\bar{F}(\bar{\mathbf{Q}})\equiv F(\mathbf{Q})$ so that the hypercrystal density $\bar{\rho}(\bar{\mathbf{r}})\equiv\bar{\rho}(\mathbf{r},\mathbf{r}^{\perp})$,

$$\bar{\rho}(\bar{\mathbf{r}})=\sum_{\bar{\mathbf{Q}}} \bar{F}(\bar{\mathbf{Q}})e^{-i\bar{\mathbf{Q}}\cdot\bar{\mathbf{r}}}, \tag{2}$$

satisfies $\rho(\mathbf{r})=\bar{\rho}(\mathbf{r},\mathbf{r}^{\perp}=0)$ by construction. As described in Ref. 15, all quantities with an overbar are defined in the hyperspace, while the quantities with a $\perp$ superscript are defined in the "inner" space, the orthogonal complement of the physical space.

Extracting information from the reconstructed quasicrystal density is difficult precisely because the density is quasiperiodic and, thus, lacks a periodically repeating unit. Even if it were possible to describe the quasicrystal as a quasiperiodic tiling, with a small number of (quasiperiodically) repeating units, it would be difficult to recognize such a tiling in the reconstructed density. Namely, like any quasiperiodic structure, quasicrystals have phase degrees of freedom, "phasons,"[24,25,29] which are realized in a quasiperiodic tiling as certain tile rearrangements.[30,31] Such tile rearrangements would produce, in principle, a dense set of partially occupied sites throughout the tiling, obscuring and diminishing the identity of the individual tiles. A similar effect could be also produced by the fluctuations in the reconstructed density caused by the experimentally imposed truncations in the sum in Eq. (1). While also affected by these limitations, the hypercrystal density given by Eq. (2) is easier to analyze since it is periodic. The hypercrystal approach can be particularly useful when investigating high symmetry local environments or when searching for an un-

derlying tiling structure. However, the hyperspace is six dimensional for i($Al_{0.570}Cu_{0.108}Li_{0.322}$) and an examination of the six-dimensional periodic i($Al_{0.570}Cu_{0.108}Li_{0.322}$) density is not a simple task. In this paper we shall resort to a visualization of the hypercrystal density in certain two- and three-dimensional planes. In addition, we shall consider projections (convolution) of the densities from regions perpendicular to the visualization planes, as well as the approximate removal (deconvolution) of thermal fluctuations from the densities. One of the main aspects of this paper will be visualization and analysis of quasicrystal densities in terms of tilings. Within a tiling picture of a quasicrystal, we shall consider averaging of reconstructed quasicrystal densities over different locations of a particular tile in a given local environment.

Let us first consider an n-dimensional subspace (plane) of the D-dimensional hyperspace, spanned by the cartesian basis $\{\hat{\mathbf{u}}_\alpha\}_{\alpha=1}^{n}, (n \leq D)$, located at $\bar{\mathbf{r}}_0$ and parametrized by $\mathbf{r}_u = \Sigma_\alpha (\mathbf{r}_u \cdot \hat{\mathbf{u}}_\alpha)\hat{\mathbf{u}}_\alpha$. Then, the hypercrystal density restricted to this plane is simply given by

$$\rho_u(\mathbf{r}_u) = \sum_{\bar{\mathbf{Q}}} \bar{F}(\bar{\mathbf{Q}}) e^{-i\bar{\mathbf{Q}}\cdot\bar{\mathbf{r}}_0} e^{-i\mathbf{Q}_u\cdot\mathbf{r}_u}, \tag{3}$$

where $\mathbf{Q}_u = \Sigma_\alpha (\bar{\mathbf{Q}}\cdot\hat{\mathbf{u}}_\alpha)\hat{\mathbf{u}}_\alpha$. On the other hand, let a subspace orthogonal to this plane be spanned by the cartesian basis $\{\hat{\mathbf{w}}_\beta\}_{\beta=1}^{m}$, $m \leq (D-n)$, and let it be parametrized by $\mathbf{r}_w = \Sigma_\beta (\mathbf{r}_w \cdot \hat{\mathbf{w}}_\beta)\hat{\mathbf{w}}_\beta$. Then, projection of the density on the $\mathbf{r}_u$ plane, from a region W of the $\mathbf{r}_w$ space, can be calculated by the following substitution in Eq. (3),

$$\bar{F}(\bar{\mathbf{Q}}) \rightarrow \bar{F}(\bar{\mathbf{Q}}) F_w(\mathbf{Q}_w), \tag{4}$$

where $\mathbf{Q}_w = \Sigma_\beta (\bar{\mathbf{Q}}\cdot\hat{\mathbf{w}}_\beta)\hat{\mathbf{w}}_\beta$ and

$$F_w(\mathbf{Q}_w) = \int_W e^{-i\mathbf{Q}_u\cdot\mathbf{r}_u} d^m r_w. \tag{5}$$

In addition, several types of disordering, including thermal phonon and phason fluctations, can be described by a Debye–Waller factor.[29] Such disordering can be approximately removed from the data by deconvoluting an overall Debye–Waller factor as follows

$$\bar{F}(\bar{\mathbf{Q}}) \rightarrow \bar{F}(\bar{\mathbf{Q}}) e^{\bar{\mathbf{Q}}\cdot\bar{\mathbf{B}}\cdot\bar{\mathbf{Q}}}, \tag{6}$$

where the tensor $\bar{\mathbf{B}}$ is obtained in the process of reconstructing the structure factors.[13,14]

In cases of interest here, we shall evaluate the density of i($Al_{0.570}Cu_{0.108}Li_{0.322}$) in the physical space $\mathbf{r}_u \equiv \mathbf{r}$ ($n = d = 3$), in the inner space $\mathbf{r}_u \equiv \mathbf{r}^\perp$ ($n = D - d = 3$), or in two-dimensional high symmetry hypercrystal planes $\mathbf{r}_u \equiv (r, r^\perp)$ ($n = 2$), located at high symmetry points $\bar{\mathbf{r}}_0$ in the hypercrystal unit cell. In addition to the projections of the two-dimensional slices of the physical space density, we shall consider projections described by Eq. (4) for the densities in the inner space, $\mathbf{r}_u \equiv \mathbf{r}^\perp$, with $\mathbf{r}_w \equiv \mathbf{r}$ and W corresponding to a small sphere. We shall also briefly mention the effect of deconvoluting thermal fluctuations using Eq. (6).

In order to be able to interpret a quasicrystal structure as a tiling, it is necessary that the tiling has the same symmetry and quasiperiodicity as the reconstructed quasicrystal density. Therefore, the reciprocal lattice and the phase relationships between the symmetry related structure factors of the tiling must be identical to those of the quasicrystal. The orientation of the tiling relative to that of the density, can be determined by matching the two reciprocal lattices. Similarly, the scale of the tiling (i.e., its "lattice constant") can be fixed, up to the well-known inflation symmetry scale factor,[32] also by matching the two reciprocal lattices.[33] Then, the relative translation between the tiling and the reconstructed density can be fixed, up to a discrete number of choices. Equivalently, the relative rotation, scale and translation needed to match the tiling to the density can be accomplished by matching of the hyperspace Wyckoff sites of the tiling and of the density. Generally, a tiling with the same symmetry and quasiperiodicity as that of the quasicrystal density in the d-dimensional physical space, can be also represented as a cut through a D-dimensional hypertiling with the same symmetry and periodicity as that of the hypercrystal.[32,34] The Wyckof sites are then defined in the usual way in the hyperspace.

Given such a tiling, we would like to calculate the density $\rho_T(\mathbf{r})$ defined as $\rho(\mathbf{r})$ averaged over all tiles of a given type T, where $\mathbf{r}$ is measured relative to a fixed point of the tile (e.g., one of its vertices, its center of symmetry, etc.). A tile type might be defined not only by its shape and orientation (a volume v_T), but also by its surrounding. Therefore, we may use the term "tile type" also to mean a particular arrangement of several tiles. Then,

$$\rho_T(\mathbf{r}) \equiv \langle \rho(\mathbf{r} + \mathbf{R}_T) \rangle, \tag{7}$$

where $\mathbf{r} \in v_T$, and $\mathbf{R}_T$ are the positions of the tiles of type T. Since each $\mathbf{R}_T$ is the physical space projection of a hyperlattice vector $\bar{\mathbf{R}}_T$, it is not difficult to prove starting from Eq. (1) that Eq. (7) reduces to

$$\rho_T(\mathbf{r}) = \sum_{\mathbf{Q}} F(\mathbf{Q}) F_T(\mathbf{Q}^\perp) e^{-i\mathbf{Q}\cdot\mathbf{r}}, \tag{8}$$

where the inner space tile form factor $F_T(\mathbf{Q}^\perp)$ can be calculated in the closed form

$$F_T(\mathbf{Q}^\perp) = \langle e^{i\mathbf{Q}^\perp\cdot\mathbf{R}_T^\perp} \rangle = \frac{1}{v_T^\perp} \int_{v_T^\perp} e^{i\mathbf{Q}^\perp\cdot\mathbf{r}^\perp} d^{D-d} r^\perp. \tag{9}$$

In cases that are of interest to us, the inner space projections $\mathbf{R}_T^\perp$ of the tile locations uniformly fill a compact domain $v_T^\perp \equiv \{\mathbf{R}_T^\perp\}$, and the above closed form is correct to order $O(N^{-1/(D-d)})$, when N, the number of tiles, is very large. Using a similar analysis, it is also possible to determine the rms variances $\sigma_T(\mathbf{r})$ of the density averaged over the tiles of a type T,

$$\sigma_T^2(\mathbf{r}) \equiv \langle [\rho(\mathbf{r} + \mathbf{R}_T) - \rho_T(\mathbf{r})]^2 \rangle. \tag{10}$$

This variance can be also written in the Fourier series form

$$\sigma_T^2(\mathbf{r}) = \sum_{\mathbf{Q}\mathbf{Q}'} F(\mathbf{Q}+\mathbf{Q}') F(-\mathbf{Q}') F_T(\mathbf{Q}^\perp) e^{-i\mathbf{Q}\cdot\mathbf{r}} - \rho_T^2(\mathbf{r}). \tag{11}$$

In the case of i($Al_{0.570}Cu_{0.108}Li_{0.322}$) we shall be interested in an icosahedral quasiperiodic tiling by the Ammann

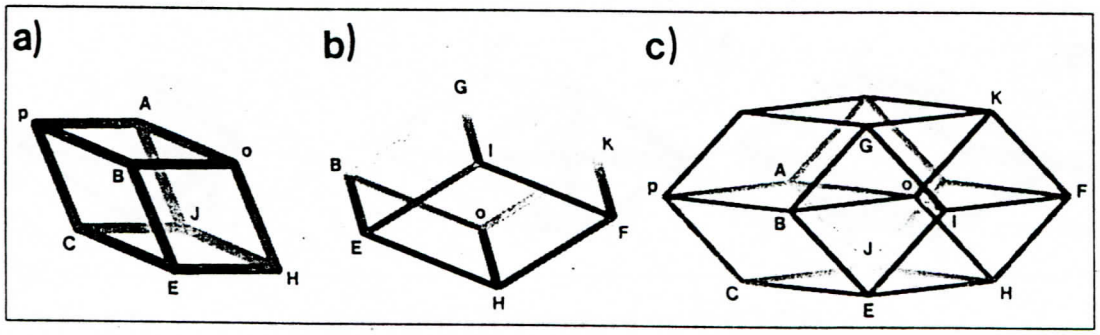

Figure 1. Ammann tiles, the prolate (a) and the oblate (b) rhombohedra, and their grouping inside a rhombic dodecahedron (c).

rhombohedra.[34–36] The above formulas, applied to the Ammann tiles in several environments, are further elaborated in the following subsection.

B. Ammann tiling

The Ammann tiling is an icosahedral quasiperiodic tiling of space[34–36] by PR and OR shown in Figs. 1(a) and 1(b). Vertices of the Ammann tiling can be obtained by a cut through a six-dimensional simple cubic hypercrystal decorated by one inner space rhombic triacontahedron (RT) per unit hypercell. In fact, these RTs are projections of unit hypercells (hypercubes) onto the inner space. Several detailed studies of local tiling configurations found in the Amman tilings have been completed.[37,38]

As described in the preceding subsection, in order to average a function over the tiles of a particular type T, it is necessary to first determine the inner space volume $v_T^\perp$ defined after Eq. (9). That is, it is necessary to determine that portion of RT which corresponds to the tile type T. Let a tiling type be specified by its "motif," a set of M vertices, $T \equiv \{\mathbf{R}_\mu\}_{\mu=1}^M$, defined relative to, say, $\mathbf{R}_1 \equiv 0$. Then, it can be easily shown that $v_T^\perp = \cap_{\mu=1}^M v_{\mathrm{RT}[\mathbf{R}_\mu^\perp]}^\perp$, where we denoted by $v_{\mathrm{RT}[\mathbf{R}^\perp]}^\perp$ the inner space RT centered at $\mathbf{R}^\perp$.[37–41] An equivalent form for evaluating $v_T^\perp$, which we shall use here, can be obtained after introducing $T_{[\mathbf{r}^\perp]}^\perp \equiv \{\mathbf{r}^\perp - \mathbf{R}_\mu^\perp\}_{\mu=1}^M$, an inner space motif associated with T and centered at some $\mathbf{r}^\perp$. Then,

$$v_T^\perp = \{\mathbf{r}^\perp | T_{[\mathbf{r}^\perp]}^\perp \in v_{\mathrm{RT}}^\perp\}, \tag{12}$$

and instead of the averaging over all occurrences of T in the tiling, one can fix T at the origin (i.e., $\mathbf{R}_1 \equiv 0$) and average over the inner space domain $v_T^\perp$ as stated in Eq. (9).

We are interested here in the following tile arrangements: PR, OR, and the rhombic dodecahedron (RD) shown in Fig. 1. Specifically, we shall consider the PR shown in Fig. 1(a) to be generated by the three vectors, denoted $\mathbf{a}_1$, $\mathbf{a}_2$, and $\mathbf{a}_3$ in Table I, that emanate from $\mathbf{R}_1 \equiv p$. In the figure, these three vectors are $pA = a\hat{\mathbf{e}}_1$, $pB = a\hat{\mathbf{e}}_2$, and $pC = a\hat{\mathbf{e}}_3$, where a is the rhombohedron edge length and $\hat{\mathbf{e}}_j$ is the unit vector in the physical space along the jth fivefold symmetry axis of the icosahedron ($j = 1,\ldots,6$). The vector $a\hat{\mathbf{e}}_j$ is simply the physical space projection of the generator $\bar{a}\hat{\mathbf{e}}_j$ of the hypercubic lattice, where $\bar{a}$ is the hypercubic lattice constant and $\hat{\mathbf{e}}_j$ is the jth cartesian basis vector in the hyperspace. The motif associated with the PR is simply the set of vertices of this PR, $T = \{p,A,B,C,o,E,J,H\}$. Using the formulas given in Eq. (12), it can be verified that the inner space domain corresponding to the PR, and denoted $v_p^\perp$, is the inner space PR shown in Fig. 2(a), generated by the three vectors $\mathbf{a}_1^\perp = a\hat{\mathbf{e}}_4^\perp = hb$, $\mathbf{a}_2^\perp = -a\hat{\mathbf{e}}_5^\perp = ha$, and $\mathbf{a}_3^\perp = a\hat{\mathbf{e}}_6^\perp = hc$, also listed in Table I, that emanate from $\mathbf{r}_0^\perp = \frac{g}{2}(\hat{\mathbf{e}}_1^\perp + \hat{\mathbf{e}}_2^\perp + \hat{\mathbf{e}}_3^\perp - \hat{\mathbf{e}}_4^\perp + \hat{\mathbf{e}}_5^\perp - \hat{\mathbf{e}}_6^\perp) = h$, where $\hat{\mathbf{e}}_j^\perp$ is the unit vector in the inner space along the jth fivefold symmetry axis of the icosahedron, and $a\hat{\mathbf{e}}_j^\perp$ is the inner space projection of the hypercu-

Table I. The inner space domain $v_{\mathrm{PR}}^\perp$. The first column lists the three vectors $\mathbf{a}_1$, $\mathbf{a}_2$, and $\mathbf{a}_3$, that emanate from the origin to generate PR in the physical space. The second column gives $\mathbf{r}_0^\perp$ from which the three vectors $\mathbf{a}_1^\perp$, $\mathbf{a}_2^\perp$, and $\mathbf{a}_3^\perp$, given in the third column, emanate to form the inner space volume $v_{\mathrm{PR}}^\perp = \mathrm{PR}^\perp$. The data that can be obtained by simple inversion are not shown.

$\mathbf{a}_1, \mathbf{a}_2, \mathbf{a}_3$	$\mathbf{r}_0^\perp$	$\mathbf{a}_1^\perp, \mathbf{a}_2^\perp, \mathbf{a}_3^\perp$
$a\hat{\mathbf{e}}_1, a\hat{\mathbf{e}}_2, a\hat{\mathbf{e}}_3$	$\frac{g}{2}(\hat{\mathbf{e}}_1^\perp + \hat{\mathbf{e}}_2^\perp + \hat{\mathbf{e}}_3^\perp - \hat{\mathbf{e}}_4^\perp + \hat{\mathbf{e}}_5^\perp - \hat{\mathbf{e}}_6^\perp)$	$a\hat{\mathbf{e}}_4^\perp, -a\hat{\mathbf{e}}_5^\perp, a\hat{\mathbf{e}}_6^\perp$
$a\hat{\mathbf{e}}_1, a\hat{\mathbf{e}}_3, a\hat{\mathbf{e}}_4$	$\frac{g}{2}(\hat{\mathbf{e}}_1^\perp - \hat{\mathbf{e}}_2^\perp + \hat{\mathbf{e}}_3^\perp + \hat{\mathbf{e}}_4^\perp - \hat{\mathbf{e}}_5^\perp + \hat{\mathbf{e}}_6^\perp)$	$a\hat{\mathbf{e}}_5^\perp, -a\hat{\mathbf{e}}_6^\perp, a\hat{\mathbf{e}}_2^\perp$
$a\hat{\mathbf{e}}_1, a\hat{\mathbf{e}}_4, a\hat{\mathbf{e}}_5$	$\frac{g}{2}(\hat{\mathbf{e}}_1^\perp + \hat{\mathbf{e}}_2^\perp - \hat{\mathbf{e}}_3^\perp + \hat{\mathbf{e}}_4^\perp + \hat{\mathbf{e}}_5^\perp - \hat{\mathbf{e}}_6^\perp)$	$a\hat{\mathbf{e}}_6^\perp, -a\hat{\mathbf{e}}_2^\perp, a\hat{\mathbf{e}}_3^\perp$
$a\hat{\mathbf{e}}_1, a\hat{\mathbf{e}}_5, a\hat{\mathbf{e}}_6$	$\frac{g}{2}(\hat{\mathbf{e}}_1^\perp - \hat{\mathbf{e}}_2^\perp + \hat{\mathbf{e}}_3^\perp - \hat{\mathbf{e}}_4^\perp + \hat{\mathbf{e}}_5^\perp + \hat{\mathbf{e}}_6^\perp)$	$a\hat{\mathbf{e}}_2^\perp, -a\hat{\mathbf{e}}_3^\perp, a\hat{\mathbf{e}}_4^\perp$
$a\hat{\mathbf{e}}_1, a\hat{\mathbf{e}}_6, a\hat{\mathbf{e}}_2$	$\frac{g}{2}(\hat{\mathbf{e}}_1^\perp + \hat{\mathbf{e}}_2^\perp - \hat{\mathbf{e}}_3^\perp + \hat{\mathbf{e}}_4^\perp - \hat{\mathbf{e}}_5^\perp + \hat{\mathbf{e}}_6^\perp)$	$a\hat{\mathbf{e}}_3^\perp, -a\hat{\mathbf{e}}_4^\perp, a\hat{\mathbf{e}}_5^\perp$
$a\hat{\mathbf{e}}_2, -a\hat{\mathbf{e}}_5, a\hat{\mathbf{e}}_3$	$\frac{g}{2}(-\hat{\mathbf{e}}_1^\perp + \hat{\mathbf{e}}_2^\perp + \hat{\mathbf{e}}_3^\perp + \hat{\mathbf{e}}_4^\perp - \hat{\mathbf{e}}_5^\perp + \hat{\mathbf{e}}_6^\perp)$	$a\hat{\mathbf{e}}_1^\perp, -a\hat{\mathbf{e}}_6^\perp, -a\hat{\mathbf{e}}_4^\perp$
$a\hat{\mathbf{e}}_3, -a\hat{\mathbf{e}}_6, a\hat{\mathbf{e}}_4$	$\frac{g}{2}(-\hat{\mathbf{e}}_1^\perp + \hat{\mathbf{e}}_2^\perp + \hat{\mathbf{e}}_3^\perp + \hat{\mathbf{e}}_4^\perp + \hat{\mathbf{e}}_5^\perp - \hat{\mathbf{e}}_6^\perp)$	$a\hat{\mathbf{e}}_1^\perp, -a\hat{\mathbf{e}}_2^\perp, -a\hat{\mathbf{e}}_5^\perp$
$a\hat{\mathbf{e}}_4, -a\hat{\mathbf{e}}_2, a\hat{\mathbf{e}}_5$	$\frac{g}{2}(-\hat{\mathbf{e}}_1^\perp - \hat{\mathbf{e}}_2^\perp + \hat{\mathbf{e}}_3^\perp + \hat{\mathbf{e}}_4^\perp + \hat{\mathbf{e}}_5^\perp + \hat{\mathbf{e}}_6^\perp)$	$a\hat{\mathbf{e}}_1^\perp, -a\hat{\mathbf{e}}_3^\perp, -a\hat{\mathbf{e}}_6^\perp$
$a\hat{\mathbf{e}}_5, -a\hat{\mathbf{e}}_3, a\hat{\mathbf{e}}_6$	$\frac{g}{2}(-\hat{\mathbf{e}}_1^\perp + \hat{\mathbf{e}}_2^\perp - \hat{\mathbf{e}}_3^\perp + \hat{\mathbf{e}}_4^\perp + \hat{\mathbf{e}}_5^\perp + \hat{\mathbf{e}}_6^\perp)$	$a\hat{\mathbf{e}}_1^\perp, -a\hat{\mathbf{e}}_4^\perp, -a\hat{\mathbf{e}}_2^\perp$
$a\hat{\mathbf{e}}_6, -a\hat{\mathbf{e}}_4, a\hat{\mathbf{e}}_2$	$\frac{g}{2}(-\hat{\mathbf{e}}_1^\perp + \hat{\mathbf{e}}_2^\perp + \hat{\mathbf{e}}_3^\perp - \hat{\mathbf{e}}_4^\perp + \hat{\mathbf{e}}_5^\perp + \hat{\mathbf{e}}_6^\perp)$	$a\hat{\mathbf{e}}_1^\perp, -a\hat{\mathbf{e}}_5^\perp, -a\hat{\mathbf{e}}_3^\perp$

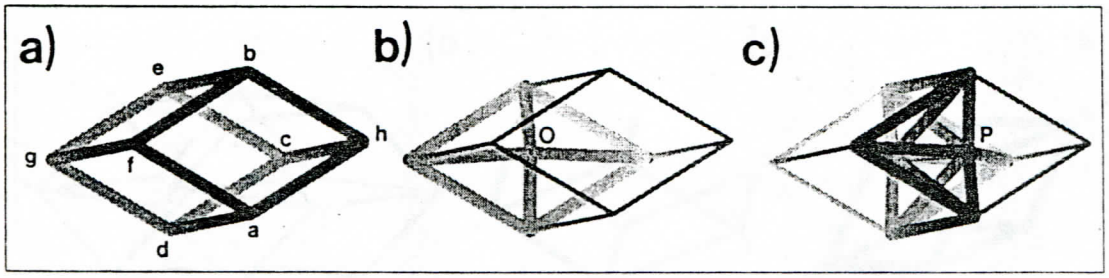

Figure 2. The PR inner space domains (a) $v_p^{\perp}$, (b) $v_{p1}^{\perp}$, and (c) $v_{p0}^{\perp}$.

bic lattice generator $a\hat{\mathbf{e}}_j$. The specific coordinates of each vertex of $v_p^{\perp}$ are listed in Table II.

Similarly, we shall consider the OR shown in Fig. 1(b) generated by the vectors $oB = -a\hat{\mathbf{e}}_1$, $oH = a\hat{\mathbf{e}}_3$, and $oK = a\hat{\mathbf{e}}_6$ that emanate from $\mathbf{R}_1 \equiv o$ and are listed in Table III. The motif associated with this OR is the set of vertices $T=\{o,B,H,K,I,E,F,G\}$. The corresponding inner space domain $v_o^{\perp}$ is the inner space OR shown in Fig. 3(a). It is generated by $ba = -a\hat{\mathbf{e}}_4^{\perp}$, $bc = -a\hat{\mathbf{e}}_5^{\perp}$, and $be = a\hat{\mathbf{e}}_2^{\perp}$ emanating from $\mathbf{r}_0^{\perp} = \frac{a}{2}(-\hat{\mathbf{e}}_1^{\perp} - \hat{\mathbf{e}}_2^{\perp} + \hat{\mathbf{e}}_3^{\perp} + \hat{\mathbf{e}}_4^{\perp} + \hat{\mathbf{e}}_5^{\perp} + \hat{\mathbf{e}}_6^{\perp}) = b$, also listed in Table III. An explicit list of the vertices of $v_o^{\perp}$ is given in Table IV.

There are 20 equivalent orientations of either PR or OR, and each can be specified by three vectors $\mathbf{a}_1$, $\mathbf{a}_2$, and $\mathbf{a}_3$ that emanate from a threefold symmetric vertex of the rhombohedron which is always taken as the origin. Similarly, the inner space domain $v_T^{\perp}$ for each of these rhombohedra is an inner space rhombohedron and can be specified by three vectors $\mathbf{a}_1^{\perp}$, $\mathbf{a}_2^{\perp}$, and $\mathbf{a}_3^{\perp}$ that emanate from its threefold symmetric vertex at $\mathbf{r}_0^{\perp}$.[37,38,40,42,43] We list $\mathbf{a}_j$, $\mathbf{r}_0^{\perp}$, and $\mathbf{a}_j^{\perp}$ in Tables I and III for ten orientations of PR and OR, respectively. The remaining ten orientations of PR and OR can be obtained by the inversion through the origin. Volumes of the existence domains are easily calculated, $v_T^{\perp} = |\mathbf{a}_1^{\perp} \cdot (\mathbf{a}_2^{\perp} \times \mathbf{a}_3^{\perp})|$, to give $v_p^{\perp} = 2\eta^3\tau^2a^3$ and $v_o^{\perp} = 2\eta^3\tau a^3$, where $\eta = 1/\sqrt{\tau+2}$ and $\tau = (1+\sqrt{5})/2$ is the golden mean. This immediately yields the numbers of the specifically oriented PR and OR per vertex of the tiling, $n_p \equiv v_p^{\perp}/v_{\mathrm{RT}}^{\perp} = \frac{1}{10}\tau^{-1}$ and $n_o \equiv v_p^{\perp}/v_{\mathrm{RT}}^{\perp} = \frac{1}{10}\tau^{-2}$, where volume of the rhombic triacontahedron is $v_{\mathrm{RT}}^{\perp} = 20\eta^3\tau^3a^3$. The integral in Eq. (9) can be easily evaluated for a rhombohedron giving

Table II. Coordinates of the vertices shown in Fig. 2 for the inner space domains $v_{\mathrm{PR}}^{\perp}$. They are expressed in the second column in terms of the rational coefficients $r_{\alpha}^{\perp}$ as $\sum_{\alpha} a r_{\alpha}^{\perp} \hat{\mathbf{e}}_{\alpha}^{\perp}$. In the third column, they are expressed in terms of the inner space cartesian coordinates $x^{\perp}$, $y^{\perp}$, and $z^{\perp}$ in the units of $a/\sqrt{\tau+2}$. We use the coordinate system of Ref. 28.

Vertex	$(r_1^{\perp},\ldots,r_6^{\perp})$	$(x^{\perp},y^{\perp},z^{\perp})$
O	(0,0,0,0,0,0)	(0,0,0)
P	(1,1,1,0,0,0)	$(2-\tau,1,0)$
a	$\frac{1}{2}(1,1,1,-1,-1,-1)$	(1,1,−1)
b	$\frac{1}{2}(1,1,1,1,1,-1)$	(1;1,1)
c	$\frac{1}{2}(1,1,1,-1,1,1)$	$(1-\tau,\tau,0)$
d	$\frac{1}{2}(1,1,1,-1,-1,1)$	$(1-\tau,0,-1)$
e	$\frac{1}{2}(1,1,1,1,1,1)$	$(1-\tau,0,1)$
f	$\frac{1}{2}(1,1,1,1,-1,-1)$	$(1,1-\tau,0)$
g	$\frac{1}{2}(1,1,1,1,-1,1)$	$(1-\tau,-\tau,0)$
h	$\frac{1}{2}(1,1,1,-1,1,-1)$	$(1,\tau+1,0)$

Table III. The inner space domain $v_{\mathrm{OR}}^{\perp}$. The first column lists the three vectors $\mathbf{a}_1$, $\mathbf{a}_2$, and $\mathbf{a}_3$, that emanate from the origin to generate OR in the physical space. The second column gives $\mathbf{r}_0^{\perp}$ from which the thee vectors $\mathbf{a}_1^{\perp}$, $\mathbf{a}_2^{\perp}$, and $\mathbf{a}_3^{\perp}$, given in the third column, emanate to form the inner space volume $v_{\mathrm{OR}}^{\perp} = \mathrm{OR}^{\perp}$. The data that can be obtained by simple inversion are not shown.

$\mathbf{a}_1,\mathbf{a}_2,\mathbf{a}_3$	$\mathbf{r}_0^{\perp}$	$\mathbf{a}_1^{\perp},\mathbf{a}_2^{\perp},\mathbf{a}_3^{\perp}$,
$-a\hat{\mathbf{e}}_1, a\hat{\mathbf{e}}_2, a\hat{\mathbf{e}}_5$	$\frac{a}{2}(-\hat{\mathbf{e}}_1^{\perp}+\hat{\mathbf{e}}_2^{\perp}+\hat{\mathbf{e}}_3^{\perp}+\hat{\mathbf{e}}_4^{\perp}+\hat{\mathbf{e}}_5^{\perp}-\hat{\mathbf{e}}_6^{\perp})$	$a\hat{\mathbf{e}}_3^{\perp}, -a\hat{\mathbf{e}}_4^{\perp}, -a\hat{\mathbf{e}}_6^{\perp}$
$-a\hat{\mathbf{e}}_1, a\hat{\mathbf{e}}_3, a\hat{\mathbf{e}}_6$	$\frac{a}{2}(-\hat{\mathbf{e}}_1^{\perp}-\hat{\mathbf{e}}_2^{\perp}+\hat{\mathbf{e}}_3^{\perp}+\hat{\mathbf{e}}_4^{\perp}+\hat{\mathbf{e}}_5^{\perp}+\hat{\mathbf{e}}_6^{\perp})$	$a\hat{\mathbf{e}}_4^{\perp}, -a\hat{\mathbf{e}}_5^{\perp}, -a\hat{\mathbf{e}}_2^{\perp}$
$-a\hat{\mathbf{e}}_1, a\hat{\mathbf{e}}_4, a\hat{\mathbf{e}}_2$	$\frac{a}{2}(-\hat{\mathbf{e}}_1^{\perp}+\hat{\mathbf{e}}_2^{\perp}-\hat{\mathbf{e}}_3^{\perp}+\hat{\mathbf{e}}_4^{\perp}+\hat{\mathbf{e}}_5^{\perp}+\hat{\mathbf{e}}_6^{\perp})$	$a\hat{\mathbf{e}}_5^{\perp}, -a\hat{\mathbf{e}}_6^{\perp}, -a\hat{\mathbf{e}}_3^{\perp}$
$-a\hat{\mathbf{e}}_1, a\hat{\mathbf{e}}_5, a\hat{\mathbf{e}}_3$	$\frac{a}{2}(-\hat{\mathbf{e}}_1^{\perp}+\hat{\mathbf{e}}_2^{\perp}+\hat{\mathbf{e}}_3^{\perp}-\hat{\mathbf{e}}_4^{\perp}+\hat{\mathbf{e}}_5^{\perp}+\hat{\mathbf{e}}_6^{\perp})$	$a\hat{\mathbf{e}}_6^{\perp}, -a\hat{\mathbf{e}}_2^{\perp}, -a\hat{\mathbf{e}}_4^{\perp}$
$-a\hat{\mathbf{e}}_1, a\hat{\mathbf{e}}_6, a\hat{\mathbf{e}}_4$	$\frac{a}{2}(-\hat{\mathbf{e}}_1^{\perp}+\hat{\mathbf{e}}_2^{\perp}+\hat{\mathbf{e}}_3^{\perp}+\hat{\mathbf{e}}_4^{\perp}-\hat{\mathbf{e}}_5^{\perp}+\hat{\mathbf{e}}_6^{\perp})$	$a\hat{\mathbf{e}}_2^{\perp}, -a\hat{\mathbf{e}}_3^{\perp}, -a\hat{\mathbf{e}}_5^{\perp}$
$a\hat{\mathbf{e}}_2, -a\hat{\mathbf{e}}_6, a\hat{\mathbf{e}}_5$	$\frac{a}{2}(-\hat{\mathbf{e}}_1^{\perp}+\hat{\mathbf{e}}_2^{\perp}-\hat{\mathbf{e}}_3^{\perp}-\hat{\mathbf{e}}_4^{\perp}+\hat{\mathbf{e}}_5^{\perp}-\hat{\mathbf{e}}_6^{\perp})$	$a\hat{\mathbf{e}}_1^{\perp}, -a\hat{\mathbf{e}}_3^{\perp}, -a\hat{\mathbf{e}}_4^{\perp}$
$a\hat{\mathbf{e}}_3, -a\hat{\mathbf{e}}_2, a\hat{\mathbf{e}}_6$	$\frac{a}{2}(-\hat{\mathbf{e}}_1^{\perp}-\hat{\mathbf{e}}_2^{\perp}+\hat{\mathbf{e}}_3^{\perp}-\hat{\mathbf{e}}_4^{\perp}-\hat{\mathbf{e}}_5^{\perp}+\hat{\mathbf{e}}_6^{\perp})$	$a\hat{\mathbf{e}}_1^{\perp}, -a\hat{\mathbf{e}}_4^{\perp}, -a\hat{\mathbf{e}}_5^{\perp}$
$a\hat{\mathbf{e}}_4, -a\hat{\mathbf{e}}_3, a\hat{\mathbf{e}}_2$	$\frac{a}{2}(-\hat{\mathbf{e}}_1^{\perp}+\hat{\mathbf{e}}_2^{\perp}-\hat{\mathbf{e}}_3^{\perp}+\hat{\mathbf{e}}_4^{\perp}-\hat{\mathbf{e}}_5^{\perp}-\hat{\mathbf{e}}_6^{\perp})$	$a\hat{\mathbf{e}}_1^{\perp}, -a\hat{\mathbf{e}}_5^{\perp}, -a\hat{\mathbf{e}}_6^{\perp}$
$a\hat{\mathbf{e}}_5, -a\hat{\mathbf{e}}_4, a\hat{\mathbf{e}}_3$	$\frac{a}{2}(-\hat{\mathbf{e}}_1^{\perp}-\hat{\mathbf{e}}_2^{\perp}+\hat{\mathbf{e}}_3^{\perp}-\hat{\mathbf{e}}_4^{\perp}+\hat{\mathbf{e}}_5^{\perp}-\hat{\mathbf{e}}_6^{\perp})$	$a\hat{\mathbf{e}}_1^{\perp}, -a\hat{\mathbf{e}}_6^{\perp}, -a\hat{\mathbf{e}}_2^{\perp}$
$a\hat{\mathbf{e}}_6, -a\hat{\mathbf{e}}_5, a\hat{\mathbf{e}}_4$	$\frac{a}{2}(-\hat{\mathbf{e}}_1^{\perp}-\hat{\mathbf{e}}_2^{\perp}-\hat{\mathbf{e}}_3^{\perp}+\hat{\mathbf{e}}_4^{\perp}-\hat{\mathbf{e}}_5^{\perp}+\hat{\mathbf{e}}_6^{\perp})$	$a\hat{\mathbf{e}}_1^{\perp}, -a\hat{\mathbf{e}}_2^{\perp}, -a\hat{\mathbf{e}}_3^{\perp}$